LAWRENCE
LIVERMORE
NATIONAL
LABORATORY

LLNL-TR-731515

Mapping of orthogonal 2D flux coordinates for two nearby magnetic X-points to logically rectangular domains

M. E. Rensink, T. D. Rognlien

May 18, 2017

Disclaimer

This work performed under the auspices of the U.S. Department of Energy by Lawrence Livermore National Laboratory under Contract DE-AC52-07NA27344.

Mapping of orthogonal 2D flux coordinates for two nearby magnetic X-points to logically rectangular domains

M.E. Rensink and T.D. Rognlien
Lawrence Livermore National Laboratory

1. Introduction

The behavior of plasmas in configurations with magnetic null points is of potential interest for a number of systems. Such nulls, sometimes referred to as X-points, a name strictly valid only for well-separated nulls where magnetic separatrices cross at a right angle, may occur in only one component of the magnetic field, such as the poloidal field in a tokamak. Numerical simulations are often used to study and predict turbulence and transport in such systems. For cases with strong magnetic field such that the ion and electron gyro-frequencies are much larger that particle collision frequencies, there is a strong anisotropy in the plasma transport along the magnetic field compared to across the field. Because of the strong anisotropy, it is often advantageous for simulations to use a coordinate system based on magnetic flux surfaces together with a coordinate orthogonal to the flux surfaces. This report presents the topological considerations needed to construct the mapping on an orthogonal flux-surface mesh onto a logically rectangular domain often used in simulation codes of the divertor region of tokamaks having two nearby X-points, thus extending the mapping now common single-null or well-separated double null-point cases with one null located at the top and bottom of the device. This extension is especially relevant to study the capability of snowflake divertors in tokamaks for reducing the peak heat flux of exhaust plasma on the target plates [1-3].

The analysis presented here follows the analytic description of the poloidal magnetic field, $B_{pol,}$ near two closely-spaced X-points given by Ryutov [1-3]. This analysis is applicable to experimental devices where the two X-points are generated by distributed poloidal field coils and the plasma core current. This analytic description is used to identify topological features of an orthogonal mesh. A key parameter that specifies the various topology changes is the poloidal angle between the primary X-point and the second X-point, and the changes are associated with a set of critical angles. Understanding these changes leads to the final step in the mesh construction by identifying the locations of various regions or patches in configuration space and in a corresponding logically rectangular index space.

UEDGE [4] and other 2-D fluid plasma simulation codes [5-7] describe the edge plasma of toroidally symmetric tokamak configurations with one or more X-points in a divertor region. The 2-D spatial mesh is usually based on a magnetic configuration produced by an MHD equilibrium code such as EFIT and written out as one or more "eqdsk" files. As illustrated in Fig. 1, the domain of the simulated plasma consists of several flux tubes bounded by poloidal magnetic flux surfaces. The number and spacing of the flux surfaces defines the "radial" resolution of the mesh. The "radial" direction is locally orthogonal to flux surfaces; the "poloidal" direction is locally parallel to flux surfaces. The "poloidal" resolution of the mesh is defined by the number of cells in the poloidal direction between adjacent flux surfaces. For boundary plasma transport codes used for tokamak configurations such as UEDGE it is convenient, though not necessary, to assume that all flux tubes have the same number of poloidal cells so the mesh is logically rectangular in index space, but does possess internal boundaries linking different sub-rectangles

in the computational domain. The following sections of this report describe indexing schemes that map tokamak magnetic configurations with one or more x-points in the divertor region(s) onto a rectangular index space. Simulation results from the UEDGE code illustrate the schemes for a few configurations.

2. Single-null and up/down double-null configurations

As an introduction to the index mapping typically used for the boundary region of magnetically diverted tokamaks, we consider a lower single-null divertor as shown in Fig, 1. The edge plasma is bounded radially by three flux surfaces: (1) an outer poloidal flux surface connecting the inboard and outboard divertor target plates; (2) an inner poloidal flux surface just inside the separatrix; and (3) a flux surface in the "private" flux (PF) region below the x-point. The edge plasma is bounded poloidally by inboard (P1) and outboard (P2) divertor plates.

The radial mesh cells are indexed from 1 to ny along the inboard divertor plate starting at the PF corner and ending at the outer wall. There are two orthogonal surfaces through the x-point; the segments in the core and PF regions define the "cut" surfaces where the poloidal indexing of the mesh is discontinuous.

The poloidal mesh cells in the common-flux region (SOL) are indexed from 1 to nx along the outer wall flux surface starting from the inboard divertor plate P1 and terminating on the outboard divertor plate

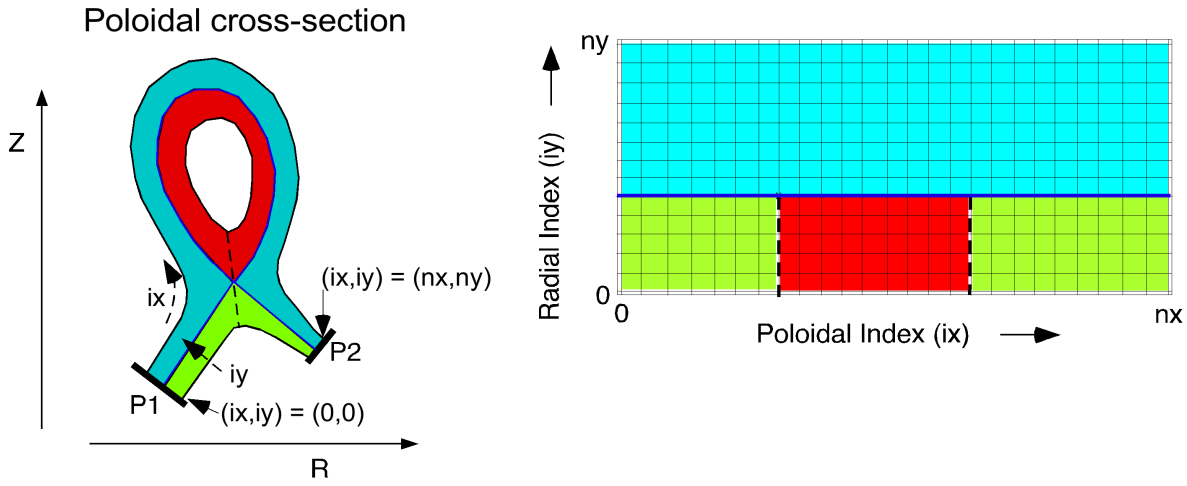

Fig. 1. Poloidal indexing of the cells in the PF region and core region is discontinuous at the "cut" defined by the orthogonal surface that originates in the PF region between plates P1 and P2 and terminates in the core region. Same colors denote the same regions in both the physical and logically rectangular domains. Upper single-null is the same as lower single-null, but with the observer position rotated 180° about the outer midplane.

The simplest double-null geometry is that where one X-point each is formed at the top and bottom of the core plasma region and are thus well separated. There are now four divertor plates shown as P1, P2, P3, and P4 in Fig. 2, where two difference magnetic flux surfaces (separatrices) pass through the two X-points. For the mesh indexing, the inner portion of the domain is represented in the left-hand rectangular domain in Fig. 2, and the outer portion of the domain is represented by the right-hand rectangle. The various indices shown in the lower figure denote values of *ix* and *iy* that internal boundaries separating the different colored regions in the physical domain

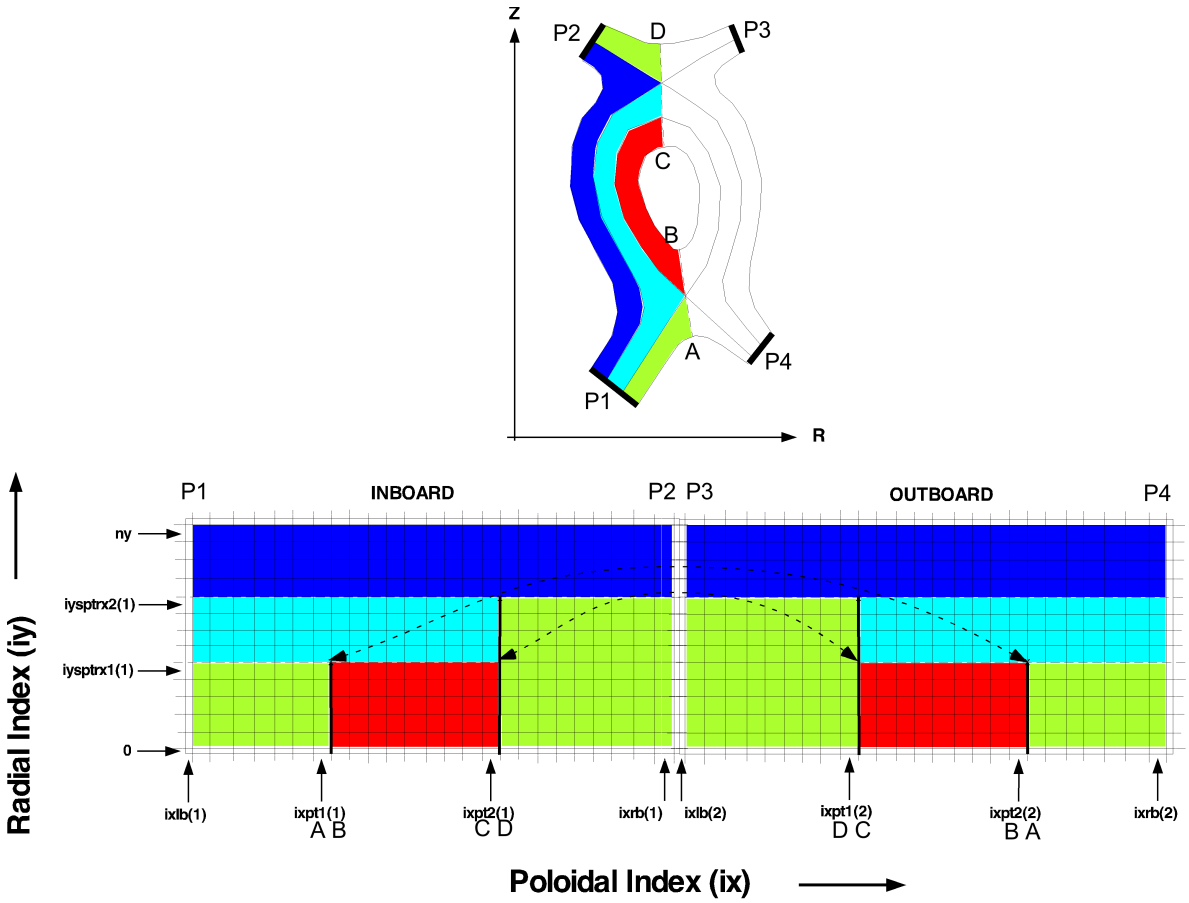

Fig. 2. Poloidal indexing of the cells in the PF region and core region is discontinuous at the "cut" defined by the orthogonal surface that originates in the PF region between plates P1 and P2 and terminates in the core region. Upper single-null is the same as lower single-null, but with the observer position rotated 180 degrees about the outer midplane.

The question address in this report is how the index mapping shown in Fig. 2 for well-separated up/down X-points changes when the two X-points are close together as in a snowflake divertor [1]. Here we detail the distinct mappings applied to orthogonal coordinates related to the snowflake-plus and snowflake-minus configurations presented in Refs. [1-3]

3. General features of orthogonal coordinates for systems with two closely-spaced X-points

Classification of various snowflake configurations is conveniently done using a power series expansion [2,3] of the poloidal magnetic flux function when two X-points are close together. As shown in these references, the topological features of snowflake flux surfaces can be characterized in terms of a single dimensionless parameter θ, which is an angle of rotation between the two X-points. However, this angle is defined in a special (x,z) orthogonal coordinate system whose origin is at the primary X-point. The (x,z) coordinate system is also rotated by another angle, say, ϕ, with respect to the standard (R,Z) orthogonal coordinate system used to describe the equilibrium poloidal flux function in tokamaks, where R is the major radius, and Z is the vertical height [1]. The degree of rotation (ϕ) between the (x,z) and (R,Z) coordinates depends on the details of the overall tokamak magnetic equilibrium that are not addressed here. We restrict ourselves to understanding the various mappings from the physical domain to a logically rectangular *ix*-*iy* index space representation commonly used for simulating edge plasmas in tokamaks as θ is varied. This procedure identifies the full range of different mappings possible and facilitates the appropriate choice of the relevant map for a given magnetic equilibrium having two nearby X-points.

Orthogonal surfaces through the X-points define the "cut" surfaces where discontinuities may occur in the poloidal indexing of the cells. There are four branches of the orthogonal surface through each X-point, but only two of these branches are "cut" surfaces. We tentatively identify these orthogonal surfaces with labels that correspond to the PF regions through which they pass.

There are six topologically different configurations for the orthogonal surfaces in the range $0° < \theta < 180°$, one for each 30º increment. There are also special snowflake configurations when θ is an exact multiple of 30º, but these are topologically unstable and will not be addressed here.

A mathematical description of the poloidal flux function in a region of two magnetic X-points is presented in Ref. [2] and extended in Ref. [3]. The model in Ref. [2] serves as the basis of the analysis presented here on how the different magnetic topologies can be represented on logically rectangular, ordered 2D flux-surface meshes in the poloidal plane often used for simulating edge plasma physics in tokamaks. Even 3D edge plasma codes often use such representations for variations in the poloidal plane.

In the region including the two X-points, following [2], an orthogonal (x, z) coordinate system is used as shown in Fig. 3. The location of first X-point, (x_1, z_1) is taken as at the origin, i.e., $(0, 0)$ and the second X-point is at (x_2, z_2). The variation of the poloidal flux function Ψ is then expressed as [2]

$$\Psi = c_1[(3z_2 - 6z)x^2 + 6x_2xz - 3z_2z^2 + 2z^3] + c_2, \quad (1)$$

where c_1 is a constant set to unity here that depends on the details of the poloidal field generation, and c_2 is simply an additive constant set to zero here; neither constant impacts the topological considerations examined in this paper. This quadratic equation gives two values of x for a given z. The shaded area above the primary X-point at (0,0) denotes the core plasma region of a tokamak

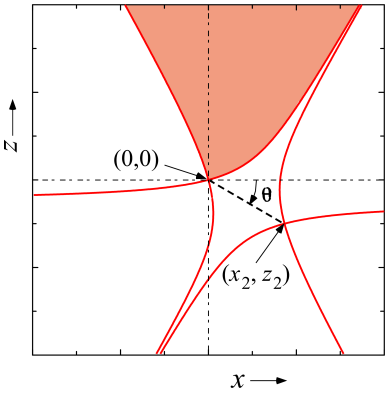

Fig. 3. Magnetic geometry considered with X-points at (x,z) = (0,0) and (x_2,z_2). Red curves are separatrices and shaded area corresponds to core-plasma region.

configuration.

The equation for the orthogonal surfaces can be obtained by differentiating Eq. (1) with respect to x to find the relation for dz/dx. Then make the replacement $dz/dx \rightarrow -\, dx/dz$ to form the differential equation for the surfaces orthogonal to Ψ, specifically

$$dx/dz = (z_2 x + x_2 z - 2xz)/(x_2 x - z_2 z - x^2 + z^2). \tag{2}$$

This equation could be simply integrated numerically to generate the second orthogonal coordinate for a flux-surface mesh based on Eq. (1). However, it turns out that Eq. (2) can be solved directly by inspection to give the algebraic relation

$$\Upsilon = (3x_2 - 6x)z^2 + 6z_2 xz - 3x_2 x^2 + 2x^3, \tag{3}$$

where Υ is a constant that labels the orthogonal surfaces. The constant of integration is also set to zero. This quadratic equation reverses the roles of (x, z) compared to that for Ψ in the sense that now there are two values of z for a given x. Thus, Eqs. (1) and (3) form a set of analytic functions for constructing an orthogonal flux-surface mesh in the vicinity of two X-points.

The separatrices shown in Fig. 3 (in red) correspond to $\Psi_1 = 0$ that passes through the origin and $\Psi_2 = z_2(3x_2^2 - z_2^2)$ that passes through the second X-point, where we use $c_1 = 1, c_2 = 0$ without loss of generality. The corresponding orthogonal surfaces (not shown in Fig. 3) that pass through the two X-points are $\Upsilon_1 = 0$ at the origin and $\Upsilon_2 = x_2(3z_2^2 - x_2^2)$.

The position of the second X-point (x_2, z_2) can conveniently be written in a polar representation introduced in Ref. [2] as $x_2 = d\, cos\, \theta$ and $z_2 = -d\, sin\, \theta$ using the distance between the X-points $d = \sqrt{(x_2^2 + z_2^2)}$ and the angle θ shown in Fig. 3. Using new expressions for x_2 and z_2, the equations for the flux surfaces becomes

$$\Psi = -(3d \sin\theta + 6z)x^2 + 6d \cos\theta\, xz + 3z^2 d \sin\theta + 2z^3, \tag{4}$$

and for the orthogonal surfaces,

$$\Upsilon = (3d \cos\theta - 6x)z^2 - 6xd \sin\theta\, z - 3d \cos\theta\, x^2 + 2x^3. \tag{5}$$

This polar representation allows one to easily identify orientation that result in a topological change of the flux surfaces as done in Ref. [2], which is augmented here by also considering the orthogonal surfaces, both of which have consequences for the mesh construction and utilization. These changes occur when the values of Ψ coincide for both X-points, and also, when the values of Υ coincide. Recall that the first X-point values are $(\Psi_1, \Upsilon_1) = (0,0)$. From Eqs. (4-5), the second X-point values are

$$(\Psi_2, \Upsilon_2) = d^3[sin\, \theta(4\, sin^2\theta - 3), -cos\, \theta(4\, cos^2\theta - 3)]. \tag{6}$$

Consequently, there will be a topological change for Ψ when $sin\, \theta(4\, sin^2\theta - 3) = 0$, correspond to $\theta = 0°, 60°,$ and $120°$ as noted by Ryutov [2]. Similarly, there are topological changes to the orthogonal surfaces when $cos\, \theta(4\, cos^2\theta - 3) = 0$, corresponding to $\theta = 30°, 90°,$ and 150, which also impacts the mapping of the physical domain to logically rectangular computation domains.

Details of the changing topologies are shown in a series of plots in Fig. 4 for a fixed $d = 1$ as the angle θ varies takes on the set of critical angles identified in the previous paragraph. Thus, each case

shown corresponds to a change in the topology of either the flux surfaces or the orthogonal surfaces. Note that the case for $\theta = 180°$ corresponds to $\theta = 0°$ with the two X-points interchanged.

For $0° < \theta < 60°$ or $180° < \theta < 120°$, the configuration is termed "snowflake-minus" in Refs. [1-3] where the separatrix of the 2nd X-point approaches the confined-plasma region. For $60° < \theta < 120°$, the 2nd X-point separatrix is well separated from the confined-plasma region, and this configuration is termed "snowflake-minus" Ref. [1-3].

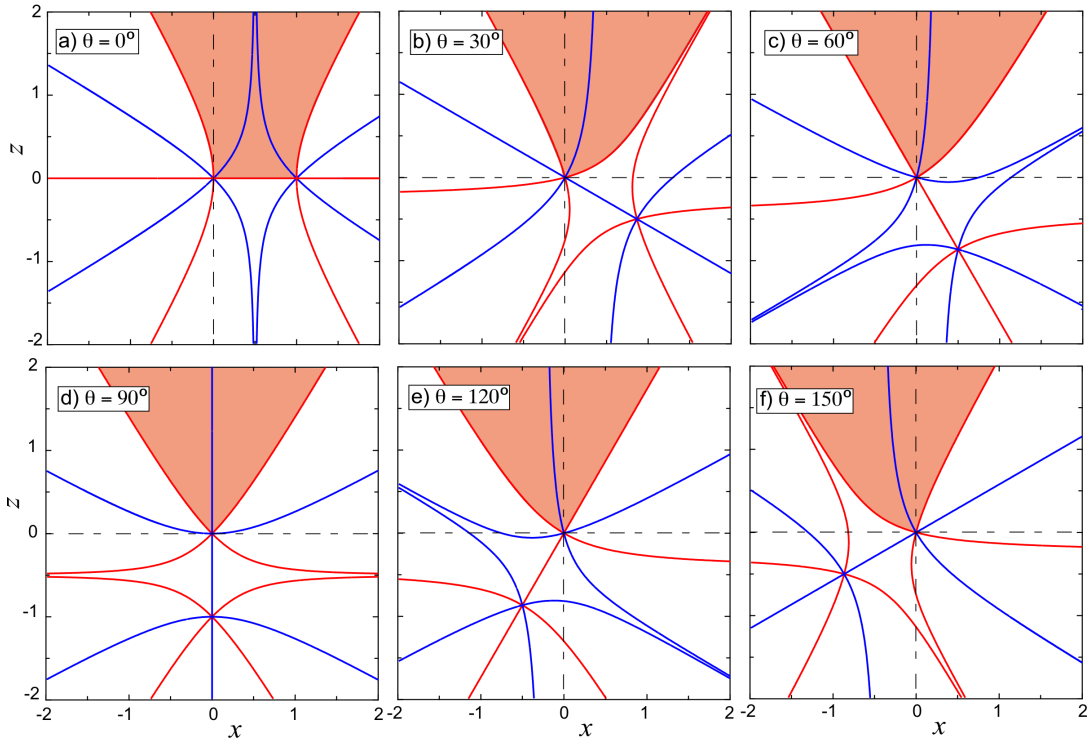

Fig. 4. Solutions showing the topology changes for flux surfaces (red) from Eq. (4) and orthogonal surfaces (blue) from Eq. (5) as the angle θ in Fig. 4 is varied. Here $(\Psi_1, \Upsilon_1) = (0,0)$ and the values of (Ψ_2, Υ_2) corresponding to $\Psi_2 = 0$ for θ=0°, 60°, and 120°, and to $\Upsilon_2 = 0$ for θ=30°, 90°, and 150°.

The change in the topology of the orthogonal surfaces is illustrated in Fig. 6 by plotting the surfaces on each side of the $\theta = 30°$ critical angle by comparing surfaces at $\theta = 29°$ to those at $\theta = 31°$. First consider the solid curves that pass through the X-points as in Fig. 5: the small region between the two

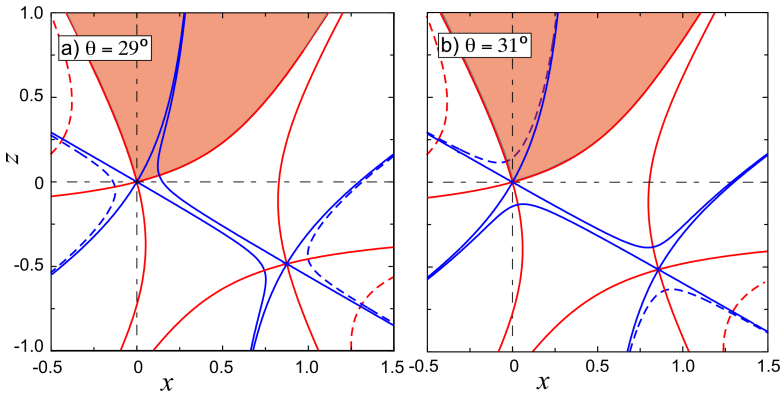

Fig. 5 Details of the orthogonal surface topology (blue) about the critical angle θ=30°. Corresponding flux surfaces are red. Dashed lines give flux and orthogonal surfaces that don't intersect X-points.

nearby orthogonal surfaces that traverse the core region (shaded) for $\theta = 29^o$ shifts to a region below $z = 0$ for $\theta = 31^o$, leaving only one orthogonal surface that traverses both an X-point and the core region. Next, consider the dashed curves that are also solutions for the two values of Ψ and two values of Υ for each θ, but they typically do not pass through the X-points and were thus omitted in Fig. 5 plots. These surfaces can be deduced from the fact that each Ψ equation is quadratic in x and each Υ equation is quadratic in z. However, the extra flux surfaces do merge into a portion of the flux surfaces shown for $\theta = 0^o$, 60^o, and 120^o, and likewise the extra orthogonal surfaces merge into a portion of the orthogonal surfaces for $\theta = 30^o$, 90^o, and 150^o. As discussed in the next section, this type of shift changes the location of various regions of the logically rectangular mesh for the orthogonal coordinate system.

4. Mapping the orthogonal mesh to a rectangular domain

Index space mapping ground rules are: (1) poloidal indexing is monotone increasing in a clockwise sense around the core plasma, but elsewhere discontinuities can occur at "cut" surfaces; (2) divertor target plates are numbered in a clockwise sense starting with P1 at the innermost plate (closest to the toroidal symmetry axis) and P2 at the outermost plate; (3) radial indexing is monotone increasing at every poloidal position, e.g., from the innermost edge plasma flux surface (nearest the core) to the outermost edge plasma flux surface (nearest the vessel wall).

a) Mapping of physical to rectangular domains for $0° < \theta < 90°$:

The first configuration covers the range $0° < \theta < 30°$, which we illustrate by the $\theta = 15°$ case in the left frame of Fig. 6. The heavy blue line corresponds to the orthogonal surface through each X-point, referred to as "cuts". One "cut" surface is the orthogonal through the primary X-point that originates in the core region and terminates in the PF region between plates P1 and P4; the other "cut" surface is the orthogonal through the secondary X-point that originates in the PF region between plates P2 and P3 and terminates in the core region.

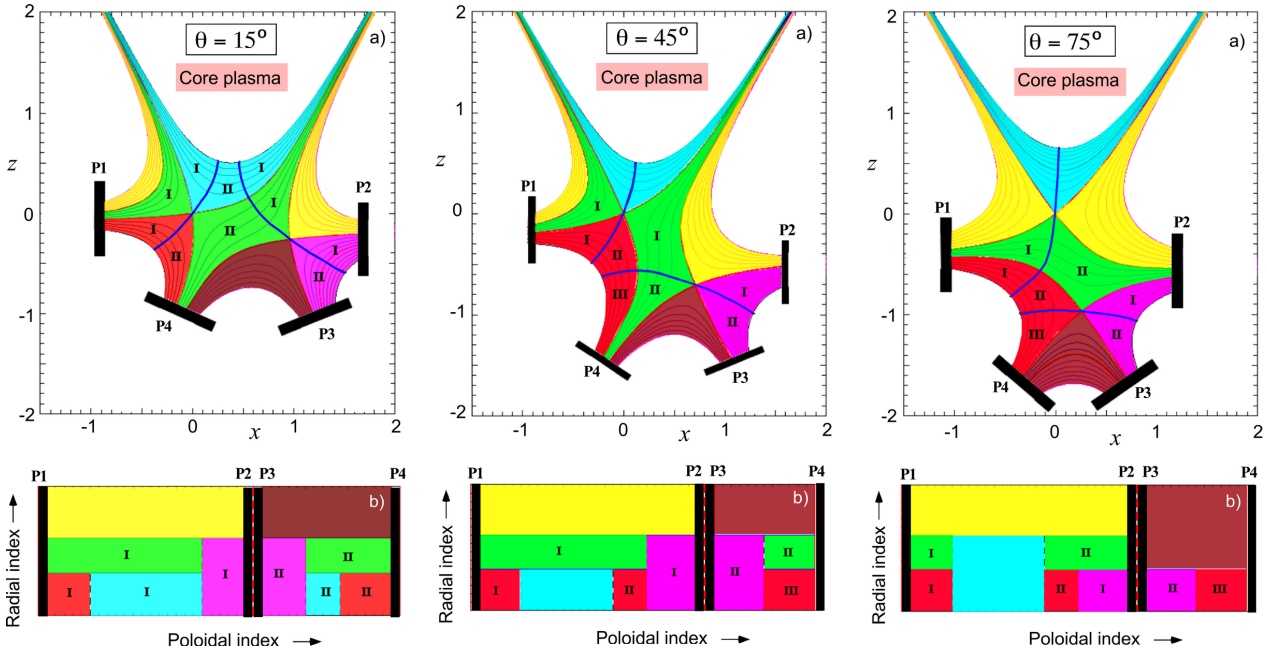

Fig. 6. Mapping of domains for orthogonal coordinates to logically rectangular domains for cases when the angle between X-points is in the range $0° < \theta < 90°$.

For the second configuration with the range $30° < \theta < 60°$, we show the $\theta = 45°$ case in center frame of Fig. 6. One "cut" surface is the orthogonal through the primary x-point that originates in the core region and terminates in the PF region between plates P1 and P4; the other "cut" surface is the orthogonal through the secondary X-point that originates in the PF region between plates P2 and P3 and terminates in the PF region between plates P1 and P4.

For the third configuration with the range $60° < \theta < 90°$, we show the $\theta = 75°$ case in the right frame Fig. 6. One "cut" surface is the orthogonal through the primary x-point that originates in the core region and terminates in the PF region between plates P1 and P4; the other "cut" surface is the orthogonal through the secondary X-point that originates in the PF region between plates P2 and P3 and terminates in the PF region between plates P1 and P4.

b) Mapping of physical to rectangular domains for $90° < \theta < 180°$:

These set of mappings can be obtained by a simple horizontal reflection of the three cases shown above for $0° < \theta < 90°$. Nonetheless, to be explicit about the different regions for the mappings to the rectangular domain, we also show the three cases in Fig. 7. The fourth configuration covers the range $90° < \theta < 120°$, with the $\theta = 105°$ case given in the left frame. One "cut" surface is the orthogonal through the primary X-point that originates in the core region and terminates in the PF region between plates P2 and P3; the other "cut" surface is the orthogonal through the secondary X-point that originates in the PF region between plates P2 and P3 and terminates in the PF region between plates P1 and P4.

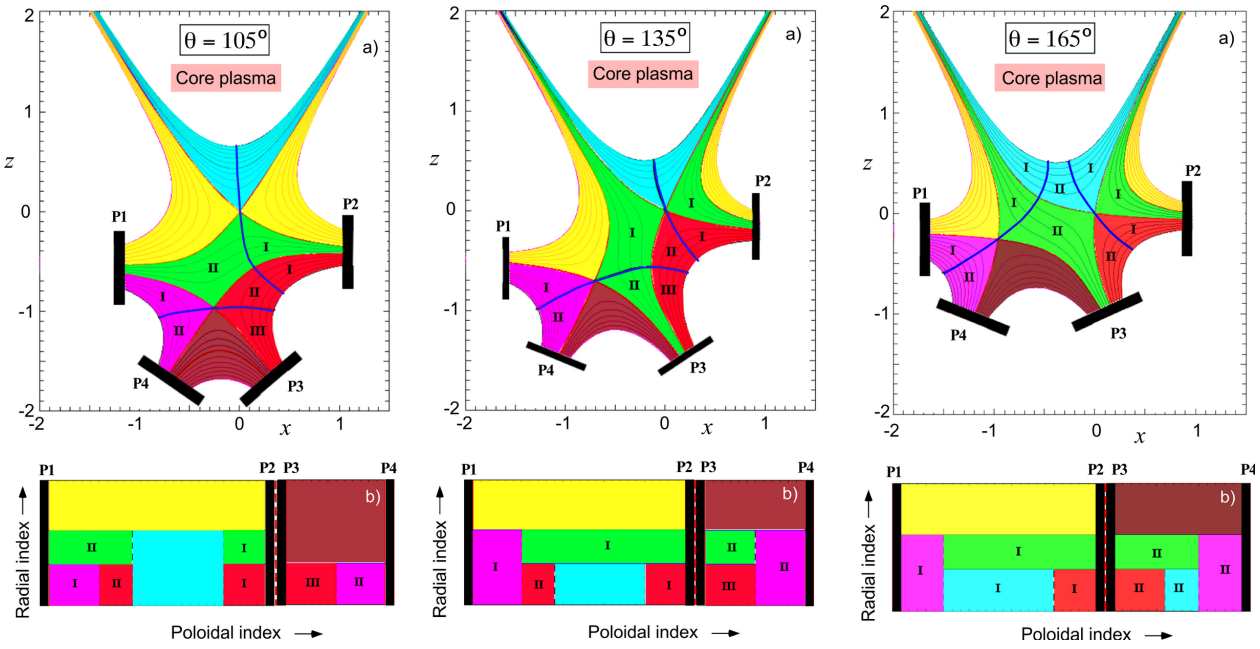

Fig. 7. Mapping of domains for orthogonal coordinates to logically rectangular domains for cases when the angle between X-points is in the range $90° < \theta < 180°$.

The fifth configuration applies to the range $120° < \theta < 150°$, which is illustrated by the $\theta = 135°$ case in the center frame of Fig. 7. One "cut" surface is the orthogonal through the primary X-point that originates in the core region and terminates in the PF region between plates P2 and P3; the other "cut" surface is the orthogonal through the secondary X-point that originates in the PF region between plates P2 and P3 and terminates in the PF region between plates P1 and P4.

Finally, the sixth configuration applies to the range $150° < \theta < 180°$, which is illustrated by the $\theta = 165°$ case in right frame of Fig. 7. One "cut" surface is the orthogonal through the primary X-point that originates in the core region and terminates in the PF region between plates P2 and P3; the other "cut" surface is the orthogonal through the secondary X-point that originates in the PF region between plates P1 and P4 and terminates in the core region.

5. Summary

This report provides a systematic scheme for mapping difference regions that can be identified for an orthogonal flux-surface mesh representation of a geometry with two magnetic X-points. The procedure utilizes the analytic representation of the flux-surfaces developed in Refs. [1-3] to describe the structure of the two X-point snowflake divertor. An equation is obtained for the surfaces orthogonal to the flux surfaces to aid in identifying when the mapping topology to a logically rectangular mesh changes as the angle θ, describing an angular rotation of the X-points is varied.

The topology of the flux surfaces described in Refs. [1-3] have three distinct regions as θ is varied from 0° to 180°. For $0° < \theta < 60°$, one has the snowflake-minus configuration; for $60° < \theta < 120°$, it is a snowflake-plus configuration; and for $120° < \theta < 180°$, it is back to a snowflake-minus. On the other hand, the mappings to a logically rectangular mesh have six distinct patterns over this range of θ, which arises because the orthogonal surfaces have topological changes in addition to the flux-surfaces. The is a connection between the two sets of mappings for $\theta < 90°$ and $\theta > 90°$, in that the latter can be obtained by a reflection of the first set about the $\theta = 90°$ axis.

Finally, it is emphasized that the orientation of $\theta = 0$ with respect to the physical (R,Z) coordinate system will depend on the nature of the poloidal flux function of the main core plasma and the primary X-point. For example, a magnetic equilibrium with high triangularity where the primary X-point is located at a significantly smaller value of R than the magnetic axis, the x-z axes will be rotated clockwise with respect to the R-Z axes. The connection between these coordinate systems can be greatly facilated by utilizing the powerful complex variable approach described in Ref. 3, by that is beyond the scope of this report.

Acknowledgements

We thank D.D. Ryutov for helpful discussions. This work was performed under the auspices of the U.S. Department of Energy by Lawrence Livermore National Laboratory under contract DE-AC52-07NA27344. This material is based upon work supported by the U.S. Department of Energy, Office of Science, Office of Fusion Energy Sciences.

References

[1] D.D. Ryutov, "Geometrical properties of a snowflake divertor," Phys. Plasmas **14** (2007) 064502.

[2] D.D. Ryutov, M.A. Makowski, and M.V. Umansky, "Local properties of the magnetic field in a snowflake divertor," Plasma Phys. Control. Fusion **52** (2010) 105001.

[3] D.D. Ryutov and V.A. Soukhanovskii, "The snowflake divertor," Phys. Plasmas **22** (2015) 110901.

[4] T.D. Rognlien and M.E. Rensink, "Edge-plasma models and characteristics for magnetic fusion energy devices," Fusion Eng. Design **60** (2002) 497.

[5] R. Schneider, X. Bonnin, K. Borass et al., "Plasma edge physics with B2-EIRENE," Contrib. Plasma Phys. **46** (2006) 3.

[6] S. Wiesen, "2006 EDGE2D/EIRENE Code Interface Report", *JET ITC Report* and http://www.eirene.de/e2deir report 30jun06.pdf.

[7] X. Bonnin, W. Dekeyser, R.A. Pitts et al., "SOLPS-ITER modeling of the Alcator C-Mod divertor plasma," Plasma Fusion Res. **11** (2016) 1403103.

Appendix I: The gridue file generated and/or used by UEDGE

Data for an externally generated mesh can be read into UEDGE via a text file "gridue". Header information in this file gives the location of the special surfaces in *ix*-*iy* index space according to the following scheme for all snowflake configurations:

First line:	nx	ny	nxpt		
Next line:	iycut1	iycut2			
Next line:	ixplate1	ixcut1	unused	ixcut2	ixplate2
Next line:	iycut3	iycut4			
Next line:	ixplate3	ixcut3	unused	ixcut4	ixplate4

All variables in this header information are integers. The poloidal dimension of the mesh is nx; the radial dimension is ny. The number of X-points in the domain is nxpt; for snowflake configurations this is always equal to 2. The divertor target plate index ixplate* is the poloidal index of the cell whose EAST face is the interface between the plasma and the "guard" cell representing each plate. The four "cut" surfaces are numbered sequentially from left to right in the poloidal direction in index space. The indices ixcut* and iycut* identify the cell whose NORTH-EAST corner coincides with the X-point at the upper terminus of each "cut" in *ix*-*iy* index space.

When this header data is read from a gridue file it is stored in variables with the following somewhat non-intuitive names (appropriate for full double-null configurations):

First line:	nx	ny	nxpt		
Next line:	iysptrx1(1)	iysptrx2(1)			
Next line:	ixlb(1)	ixpt1(1)	unused	ixpt2(1)	ixrb(1)
Next line:	iysptrx1(2)	iysptrx2(2)			
Next line:	ixlb(2)	ixpt1(2)	unused	ixpt2(2)	ixrb(2)

Indirect addressing in the poloidal (*ix*-direction) of the mesh in UEDGE is implemented by defining the arrays ixm1(ix,iy) and ixp1(ix,iy). The radial (*iy*-direction) of the mesh does not use indirect addressing.